

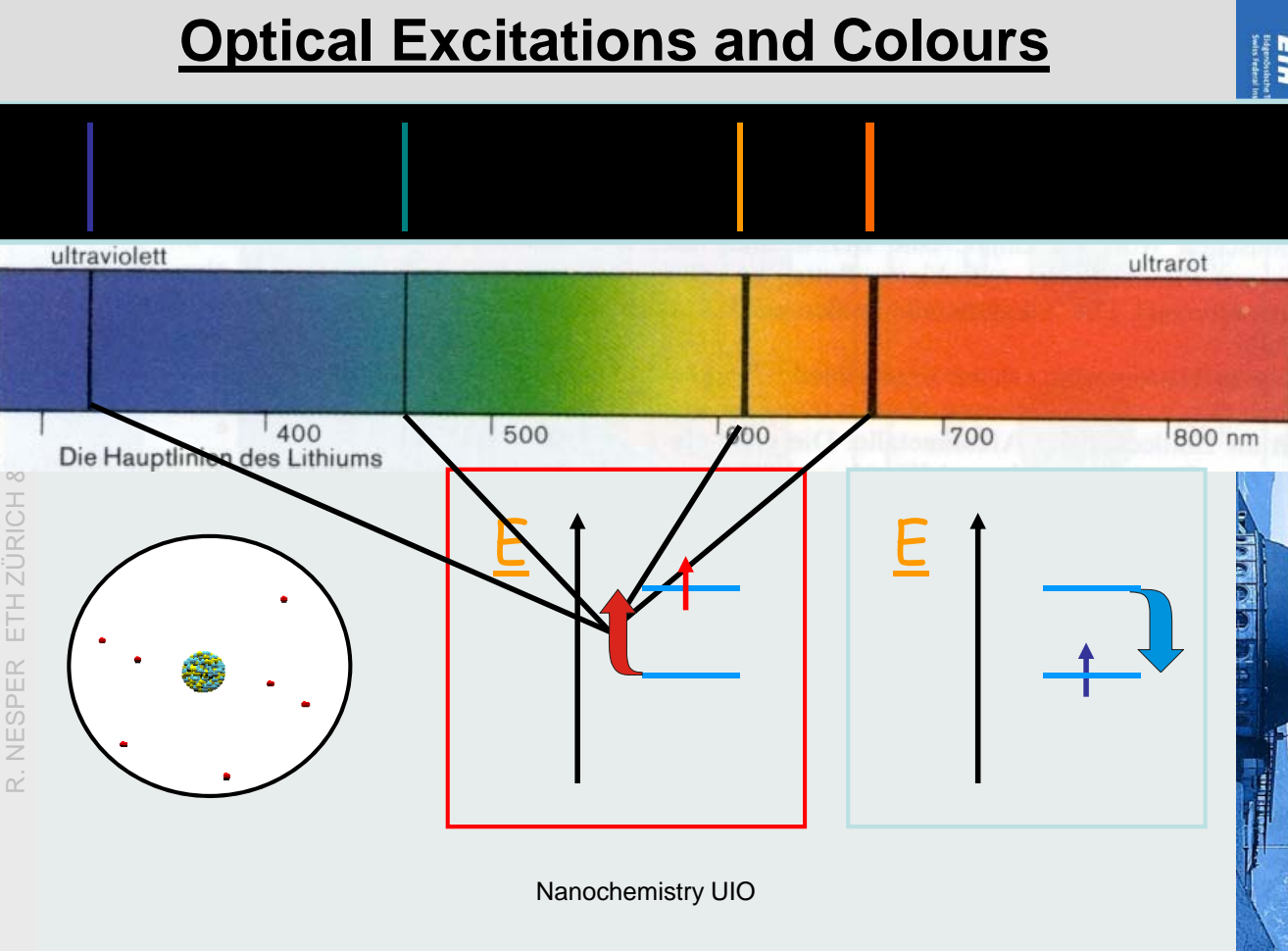
Searching New Materials for Energy Conversion and Energy Storage

1. Renewable Energy
2. Solar Cells
3. Thermoelectricity
4. Fast High Energy Li-Ion Batteries
5. Light Emitting Devices
6. Hydrogen Storage
7. Luminescent Materials
8. New Materials

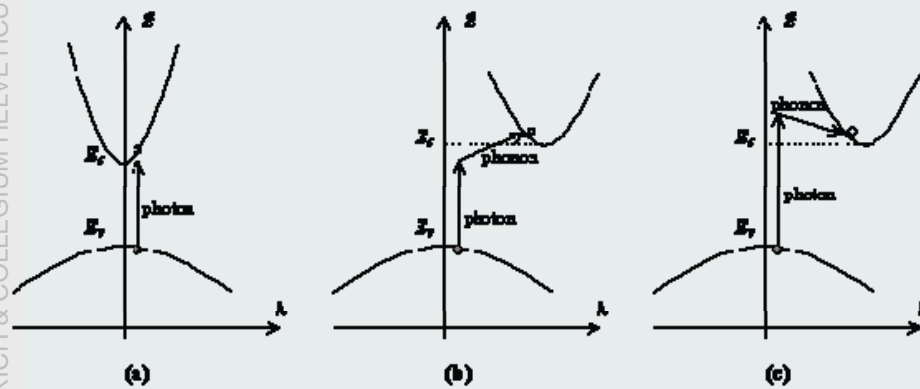
22.10.2008

Nanochemistry UIO

1



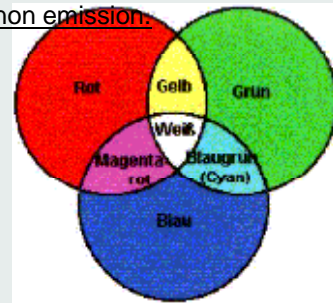
Light absorption and -emission



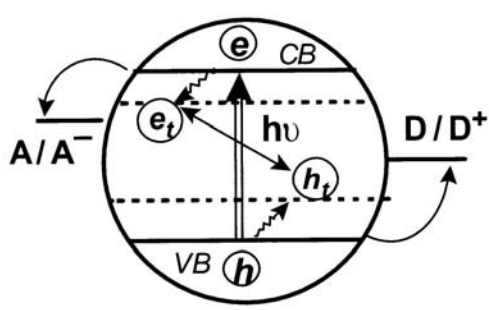
E-k diagram illustrating

- (a) Photon absorption in a direct bandgap semiconductor
- (b) Photon absorption in an indirect bandgap semiconductor assisted by phonon absorption
- (c) Photon absorption in an indirect bandgap semiconductor assisted by phonon emission

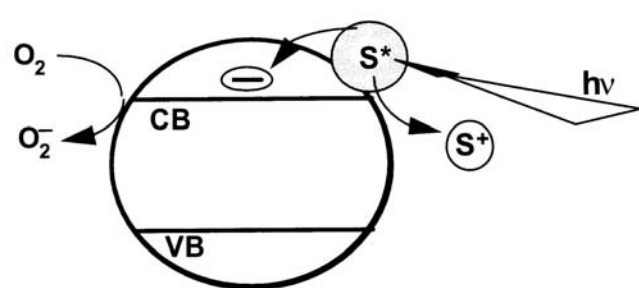
Nanochemistry UIO



Excitation and Charge Separation



(a)



(b)

Fig. 19.1. Photoinduced charge transfer processes in semiconductor nanoclusters. (a) Under bandgap excitation and (b) sensitized charge injection by exciting adsorbed sensitizer

(S). CB and VB refer to the conduction and valence bands of the semiconductor and e_t and h_t refer to trapped electrons and holes, respectively.

Electron – hole separation for avoiding quenching or recombination of charges

Nanochemistry UIO

Solar Energy

"At some point, almost certainly within this decade, we will peak in the amount of oil that is produced worldwide."

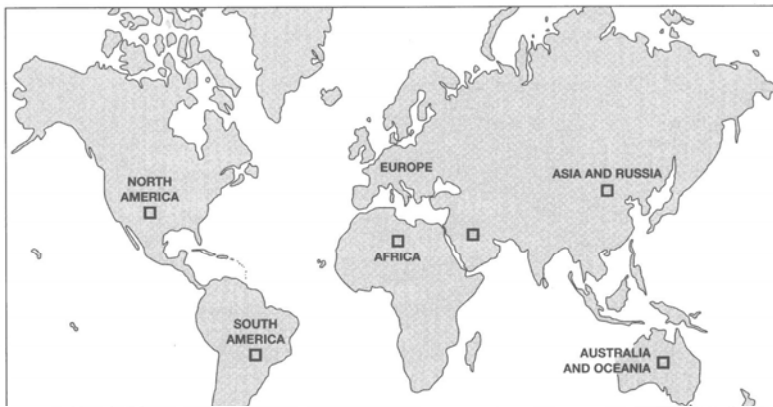
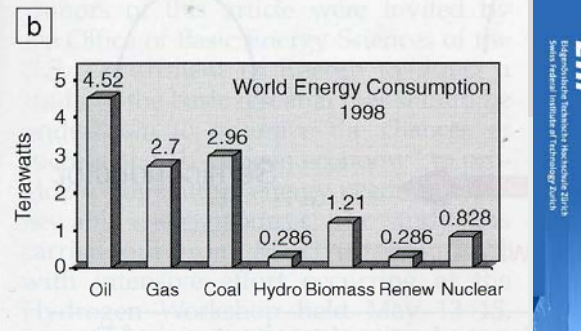


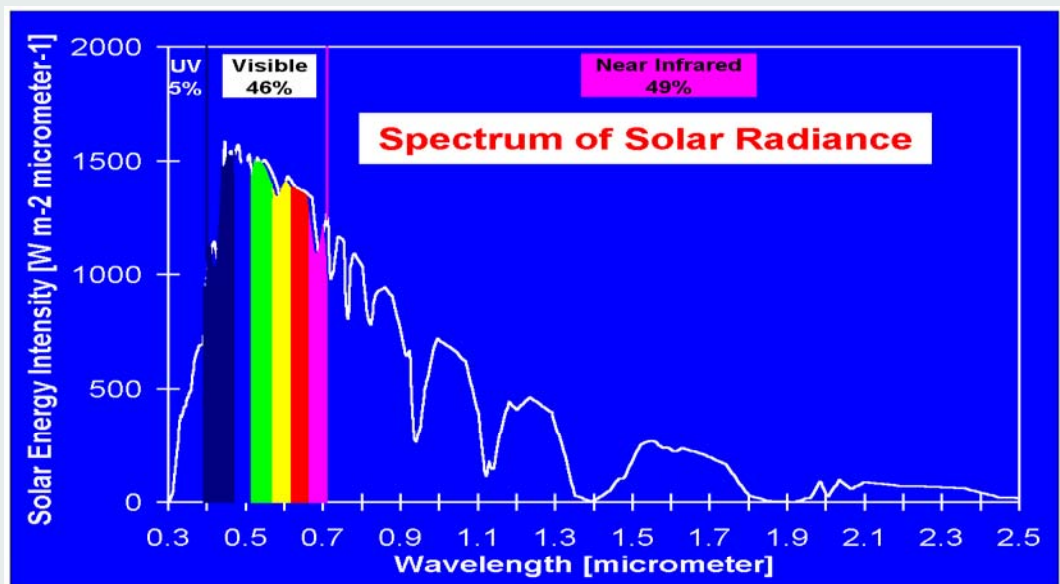
Figure 3. Solar cell land area requirements in which the six boxes (100 km on a side), located in areas of high solar radiation, can each provide 3.3 terawatts of electrical power to a total of ~20 terawatts of electrical power. Courtesy of Nate Lewis of the California Institute of Technology.

"To give all 10 billion people on the planet the level of energy prosperity we in the developed world are used to, a couple of kilowatt-hours per person, we would need to generate 60 terawatts around the planet—the equivalent of 900 million barrels of oil per day."

Searching New Materials for Energy Conversion and Energy Storage

1. Renewable Energy
2. Solar Cells
3. Thermoelectricity
4. Fast High Energy Li-Ion Batteries
5. Light Emitting Devices
6. Hydrogen Storage
7. Luminescent Materials
8. New Materials

Solar Energy Spectrum



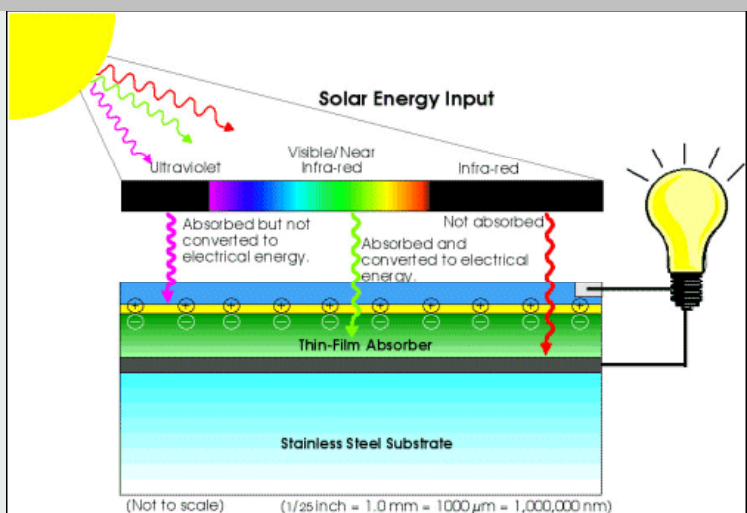
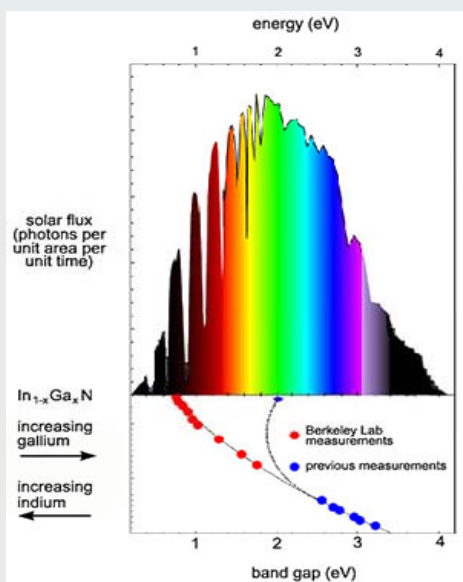
- Power reaching earth 1.37 kW/m^2

22.10.2008

Nanochemistry UIO

7

Solar Cells - Better than Biology ?



A newly established low band gap for indium nitride means that the indium gallium nitride system of alloys ($\text{In}_{1-x}\text{Ga}_x\text{N}$) covers the full solar spectrum

22.10.2008

Nanochemistry UIO

8

Solar cell – Working Principle

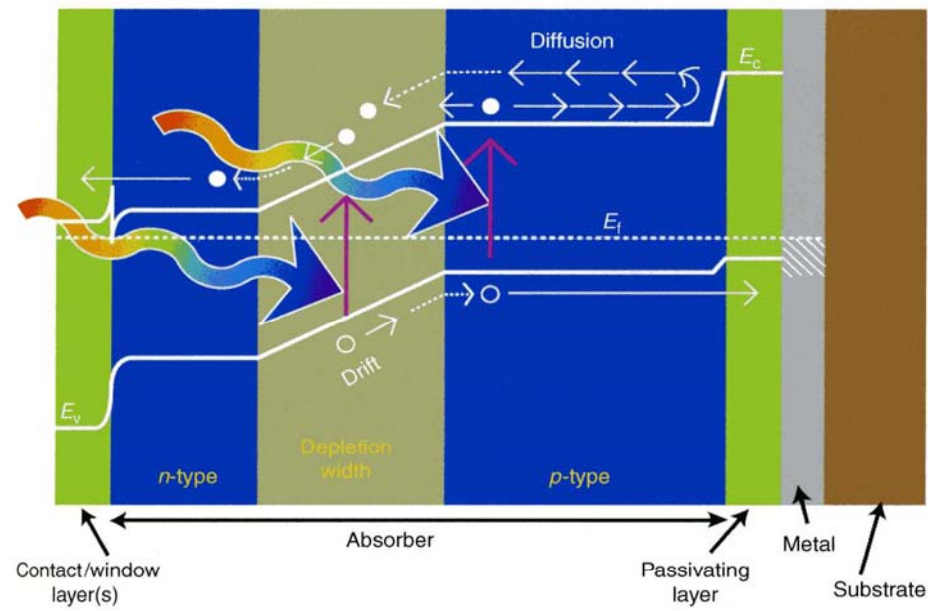


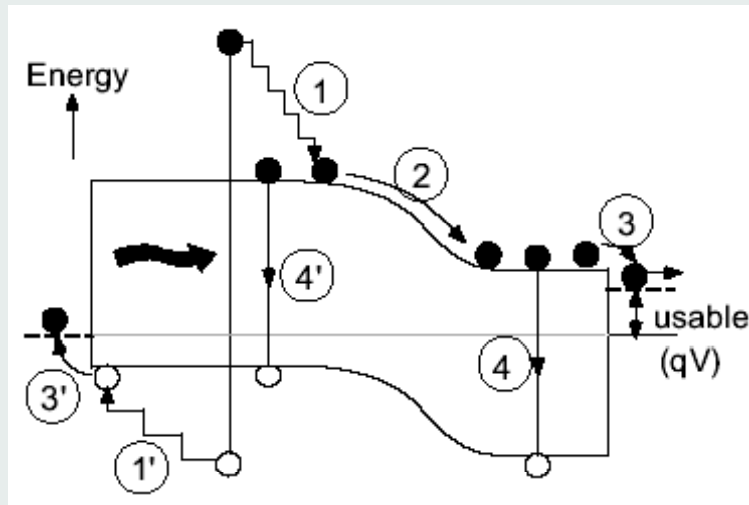
Figure 4. Schematic illustration of a $p-n$ junction solar cell, showing the structure, carrier generation, and separation. Wavy arrows represent photons. E_v is the valence-band energy, E_f is the Fermi level, and E_c is the conduction-band energy. (Courtesy of S. Kurtz.)

22.10.2008

Nanochemistry UIO

9

Efficiency Losses in Solar Cell



1 = Thermalization loss

2 and 3 = Junction and contact voltage loss

4 = Recombination loss

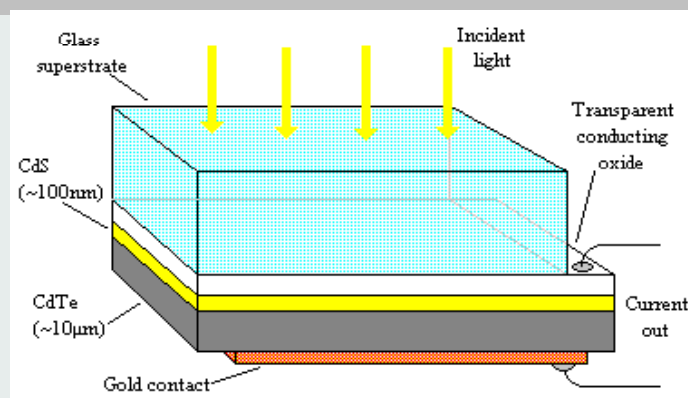
After Y. Wakchaure: http://www.nd.edu/~gsnider/EE698A/Yogesh_Solar_cells.ppt

22.10.2008

Nanochemistry UIO

10

CdTe/CdS Solar Cell



- CdTe : Bandgap 1.5 eV; Absorption coefficient 10 times that of Si
- CdS : Bandgap 2.5 eV; Acts as window layer

Limitation :

Poor contact quality with p-CdTe ($\sim 0.1 \Omega\text{cm}^2$)

After Y. Wakchaure: http://www.nd.edu/~gsnider/EE698A/Yogesh_Solar_cells.ppt

22.10.2008

Nanochemistry UIO

11

Solar Cells with Antennas

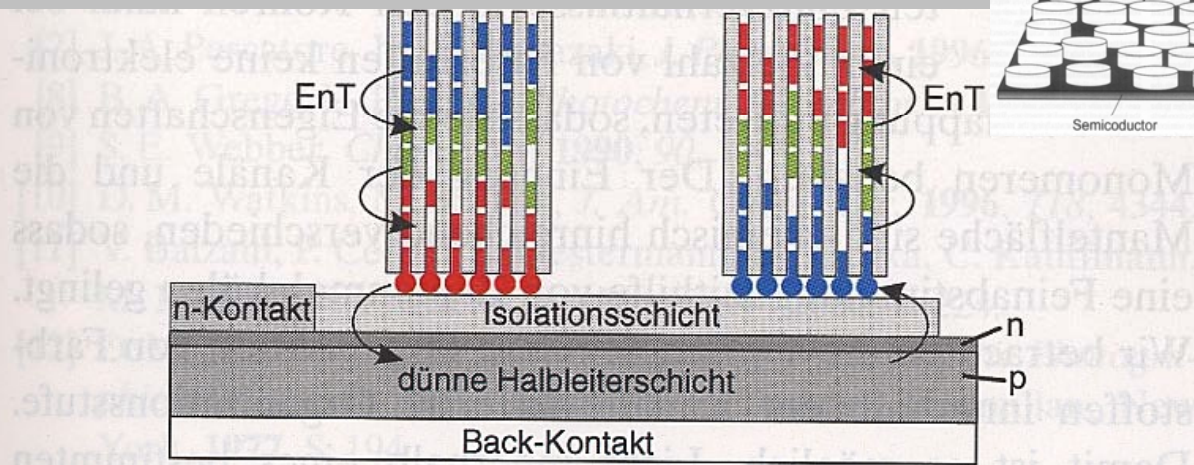


Abbildung 32. a) Prinzip einer antennensensibilisierten Solarzelle, in der der Halbleiter als EnT-Acceptor fungiert. b) Prinzip einer LED, bei der der Halbleiter als Energieübertragungs-Donor fungiert. Die Energie wird in beiden Fällen strahlungslos übertragen.

Antenna Performance (Calzaferri System)

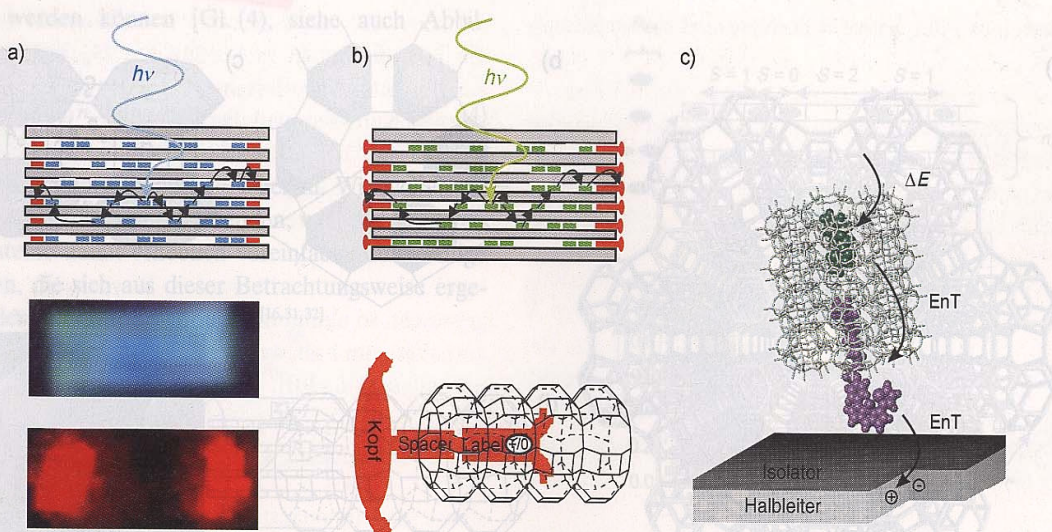
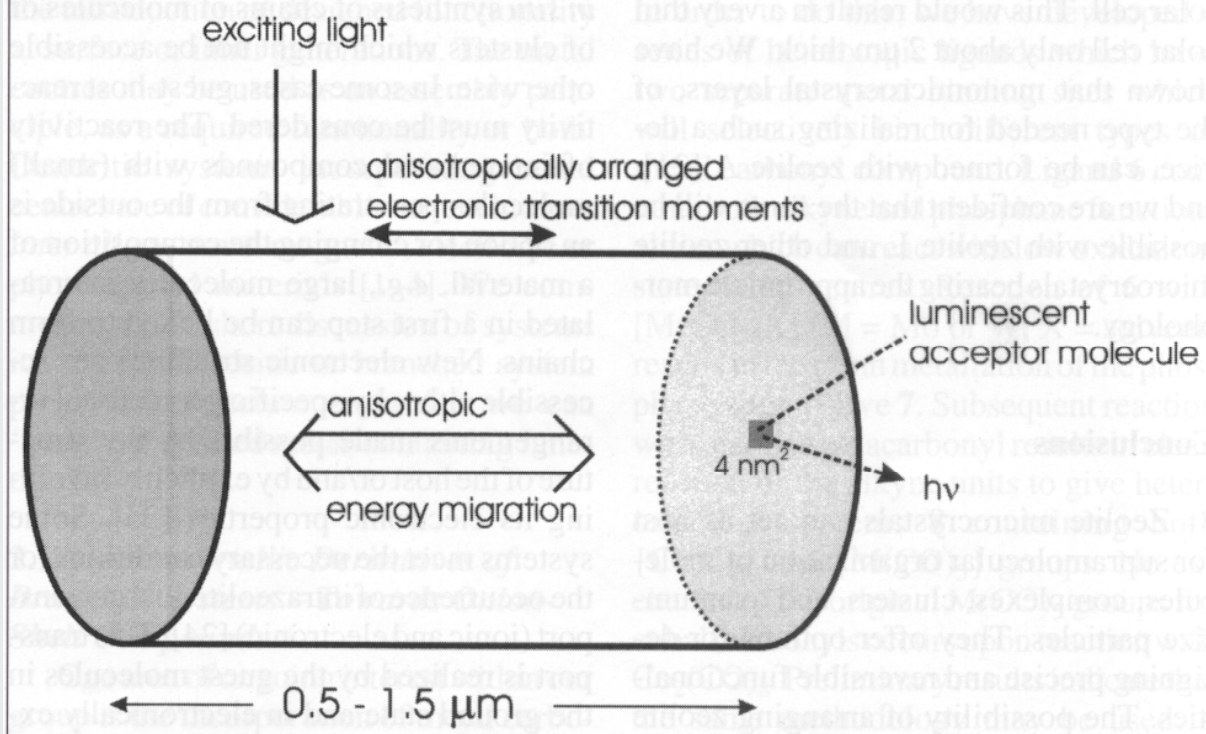


Abbildung 2. a) Farbstoffbeladene Zeolith-L-Antenne. Blau-emittierende Donoren im Innern von Zeolith L übertragen ihre elektronische Anregungsenergie zu rot-emittierenden Aczeptoren an den beiden Enden des zylinderförmigen Kristalls. In der Mitte und unten ist eine fluoreszenzmikroskopische Aufnahme eines etwa 2000 nm langen Kristalls gezeigt, der im mittleren Bereich DMPO enthält (blau, Polarisator parallel) und an den beiden Enden Ox^+ (rot, Polarisator senkrecht), bei selektiver Anregung von DMPOPOP. b) Antennensystem mit Zapfenmolekülen, die als externe Fänger wirken, an den Enden der Kanäle; wie unten dargestellt, besteht das Zapfenmolekül aus einem Kopf, einem Spacer und einem Label. c) Strahlungslose Energieübertragung (EnT) von einer photonischen Antenne auf einen Halbleiter unter Erzeugung eines Elektron-Loch-Paares.

Functional Inorganics SS2006 R.
Nesper

13

Energy Transport in Zeolite Channels (Calzaferri System)



Functional Inorganics SS2006 R.
Nesper

14

Antenna Construction (Calzaferri System)

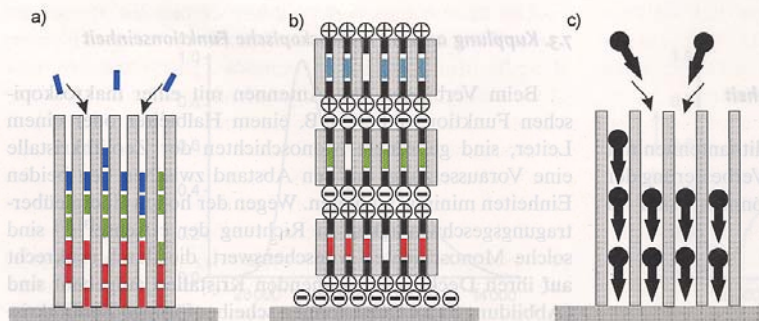


Abbildung 31. Aufbau von monodirektionalen Antennensystemen: a) aufeinanderfolgender Einbau in einen fixierten Zeolithkristall; b) schichtweiser Aufbau von Kristallen, die mit unterschiedlich geladenen Zapfen modifiziert wurden; c) Einbau von nichtzentrosymmetrischen Farbstoffen, die jeweils mit dem gleichen Ende in die Kanäle eintreten.

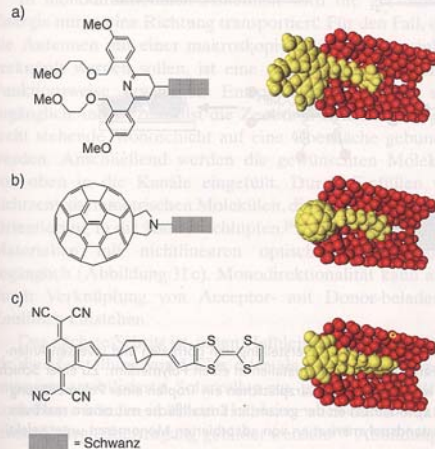


Abbildung 29. Beispiele für Zapfenmoleküle. Die Kalottenmodelle der aufgeschnittenen Kanäle mit Zapfenmolekülen illustrieren die Größenverhältnisse. a) fluoreszierender Chemosensor, b) C₆₀-Zapfen, c) molekularer Gleichrichter als Zapfenmolekül.

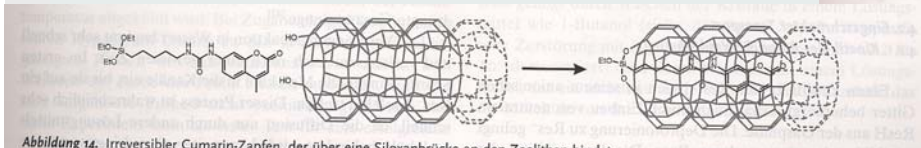


Abbildung 14. Irreversibler Cumarin-Zapfen, der über eine Siloxanbrücke an den Zeolithen bindet.

Angew. Chem. 2003, 115, 3860–3888

[www.angewandte.de](http://www angewandte de)

© 2003 Wiley-VCH Verlag GmbH & Co. KGaA, Weinheim



Antenna Organization (Calzaferri System)

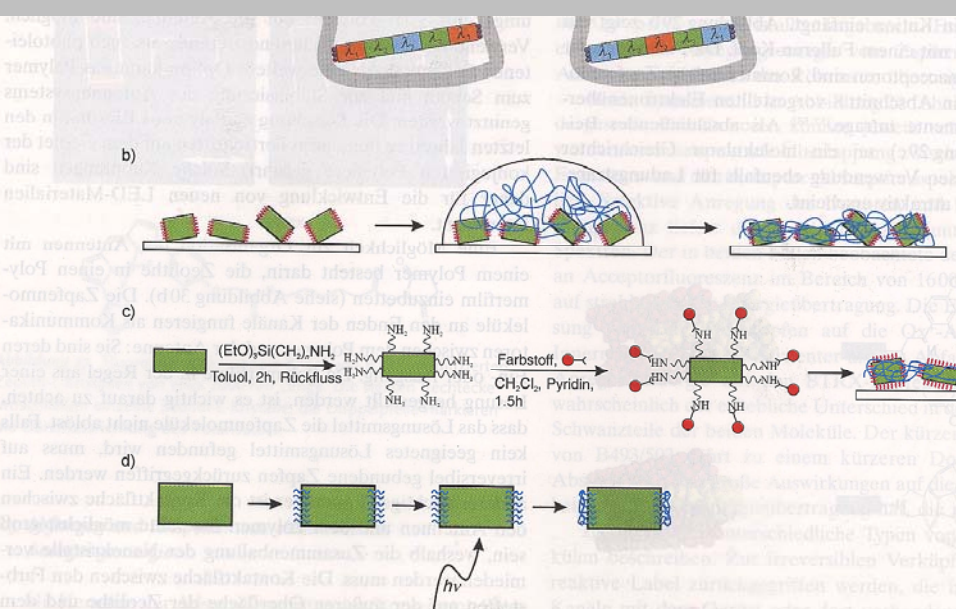


Abbildung 30. a) Kupplung eines bidirektionalen Farbstoff-Zeolith-L-Materials an ein Polymer zur Herstellung von normalen und inversen Antennensystemen. Das Polymer ist als graues Band dargestellt. b) Einlagerung von Farbstoff-Zeolith-L-Kristallen in einen Polymerfilm: Zu einer Schicht von Farbstoff-Zeolith-L-Kristallen, die mit Zapfenmolekülen modifiziert wurden, wird auf einem Quarzplättchen ein Tropfen einer Polymerlösung gegeben. Das Lösungsmittel wird verdampft und zurück bleibt ein Polymerfilm. c) Modifikation der gesamten Kristallfläche mit einem reaktiven Farbstoff zur Erzeugung einer maximalen Kontaktfläche zum Polymer. d) Festzustandspolymerisation von adsorbierten Monomeren unter selektiver Bindung der Polymere an die Deckflächen.



Solar Cells – Grätzel Cell

Dye-Sensitized Solid-State Heterojunction Solar Cells

Michael Grätzel

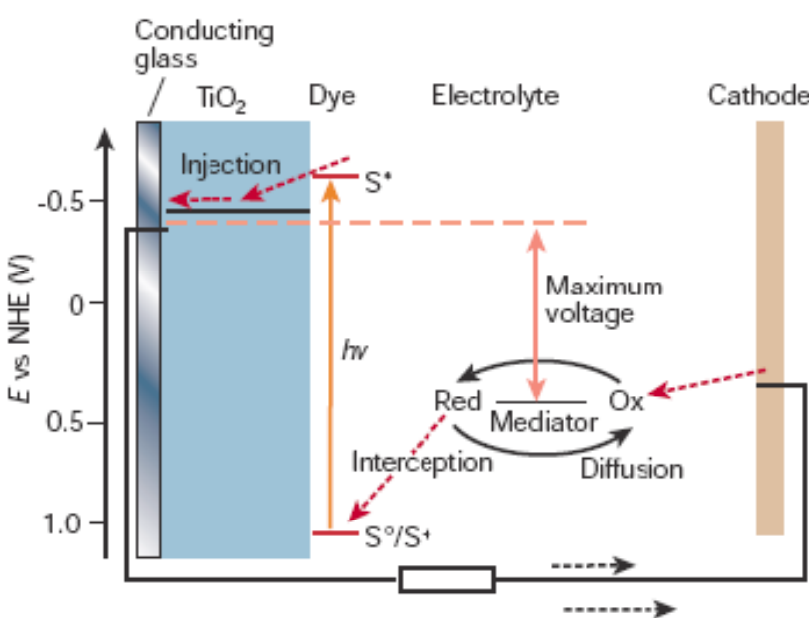
The dye-sensitized solar cell (DSSC) provides a technically and economically viable alternative concept to present-day *p–n* junction photovoltaic devices. In contrast to conventional silicon systems, where the semiconductor assumes both the task of light absorption and charge carrier transport, these two functions are separated in DSSCs. The use of sensitizers having a broad absorption band in conjunction with wide-bandgap semiconductor films of mesoporous or nanocrystalline morphology permits harvesting a large fraction of sunlight. There are good prospects that these devices can attain the conversion efficiency of liquid-electrolyte-based dye-sensitized solar cells, which currently stands at 11%. In this article, we present the current state of the field, the realm of our review being restricted to the discussion of organic molecular hole conductors, which have demonstrated the best performance to date.

22.10.2008

Nanochemistry UIO

17

Solar Cell after M. Grätzel

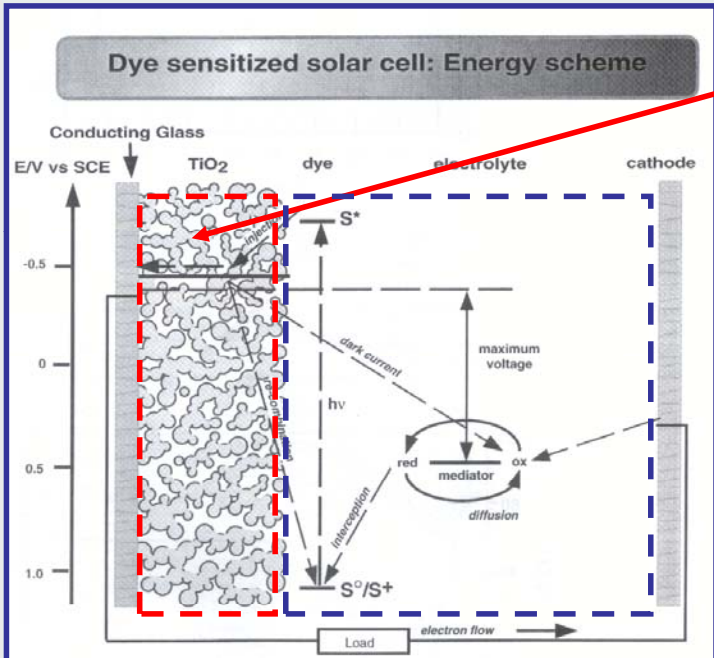


22.10.2008

Nanochemistry UIO

18

Grätzel Cell – Liquid Electrolyte - Working Principle



Nanoscopic TiO₂
– spherical particles

Electron excitation on dye
– Ru-complexes
– Ru²⁺ → Ru³⁺

Electron injection &
conduction to electrode

– TiO₂ conduction band
– percolation through
TiO₂ packing

Hole injection at dye
– Ru³⁺ + I⁻ → Ru²⁺ + I⁻

Hole transport to cathode
– I⁻ + I₂ diffusion

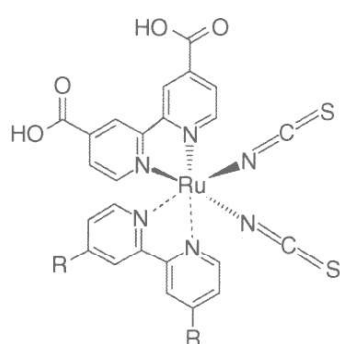
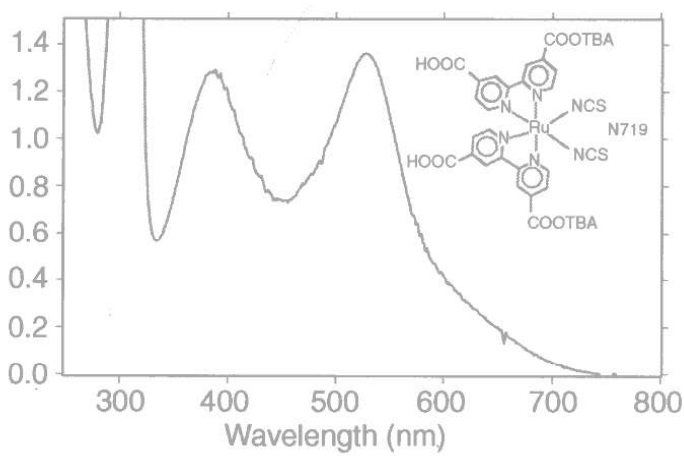
cathode reaction
– I₂ + 2e⁻ → 2I⁻

22.10.2008

Nanochemistry UIO

19

Grätzel Cell – Electron Excitation - Dye



Long alkyl chains extent
into hydrophobic organic
hole conductor

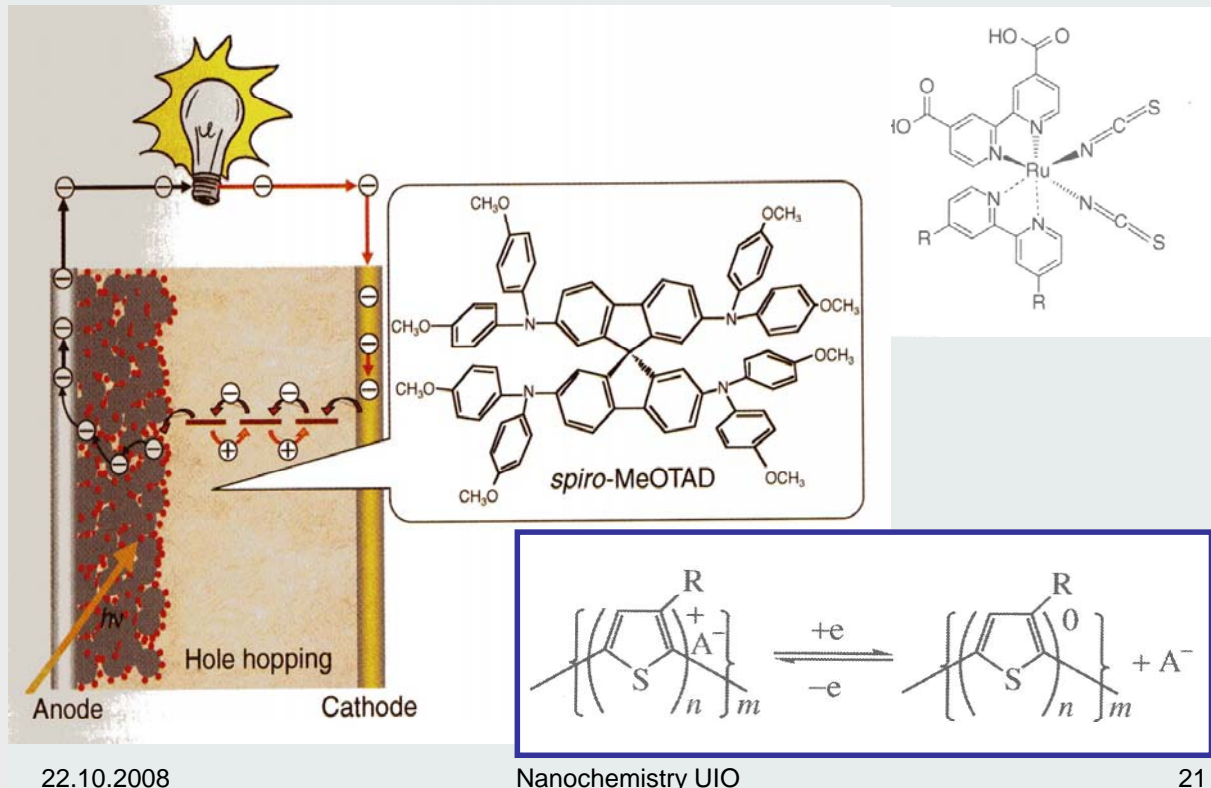
Electron excitation on dye → MLCT type

22.10.2008

Nanochemistry UIO

20

DSS Cell – Non-liquid Hole Conductor

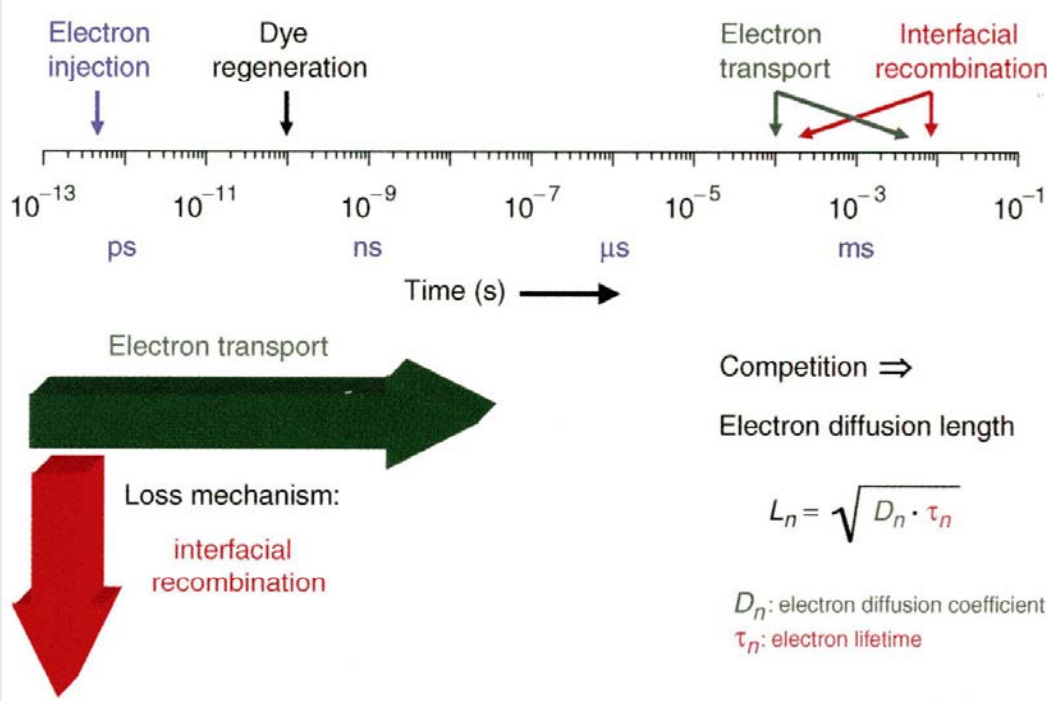


22.10.2008

Nanochemistry UIO

21

DSS-Cell – Time Scales – Loss Processes

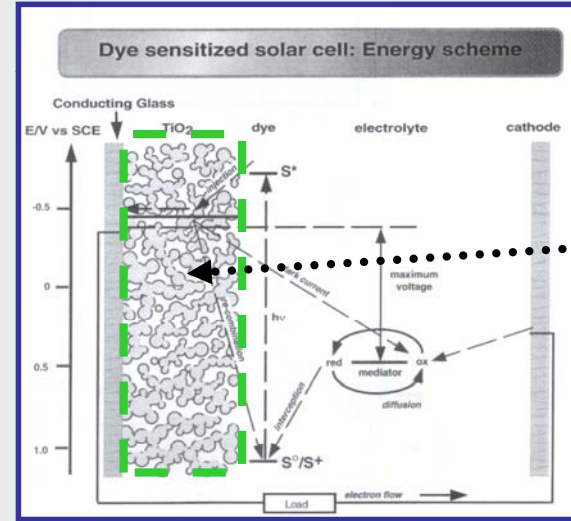


22.10.2008

Nanochemistry UIO

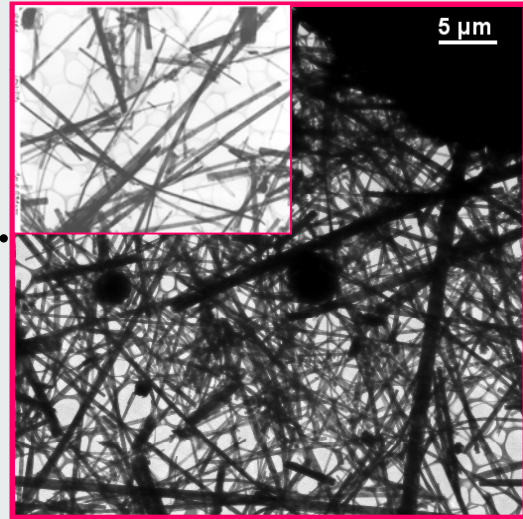
22

Grätzel Cell – Possible Enhancement



TiO₂ – Nano Fibers

energy conversion efficiency can rise to 33% in theory



better percolation = higher efficiency

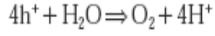
22.10.2008

Nanochemistry UIO

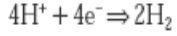
23

Tandem Cell for Water Cleavage

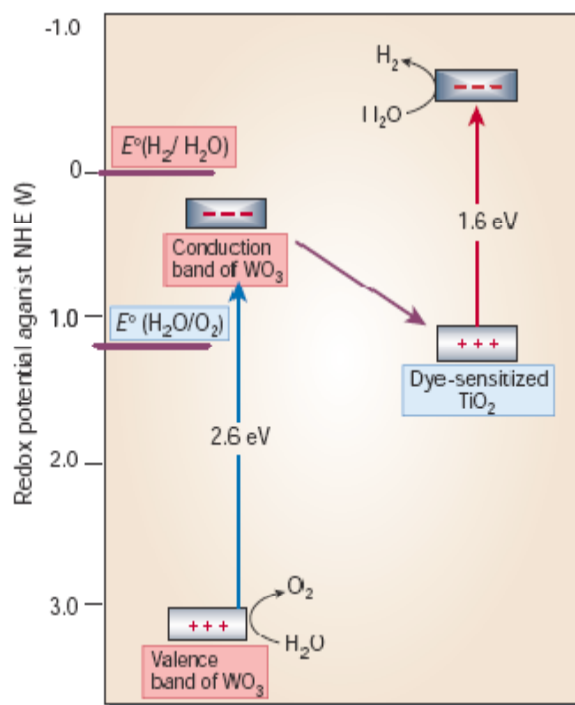
Based on two photosystems connected in series as shown in the electron flow diagram: A thin film of nanocrystalline tungsten trioxide, WO₃ (ref. 34), or Fe₂O₃ (ref. 35) serves as the top electrode absorbing the blue part of the solar spectrum. The valenceband holes (h⁺) created by band-gap excitation of the film oxidize water to oxygen:



and the conduction-band electrons are fed into the second photosystem consisting of the dye-sensitized nanocrystalline TiO₂ cell discussed above. The latter is placed directly under the WO₃ film, capturing the green and red part of the solar spectrum that is transmitted through the top electrode. The photovoltage generated by the second photosystem enables hydrogen to be generated by the conduction-band electrons.



The overall reaction corresponds to the splitting of water by visible light. There is close analogy to the 'Z-scheme' (named for the shape of the flow diagram) that operates in photosynthesis. In green plants, there are also two photosystems connected in series, one that oxidizes water to oxygen and the other generating the compound NADPH used in fixation of carbon dioxide.



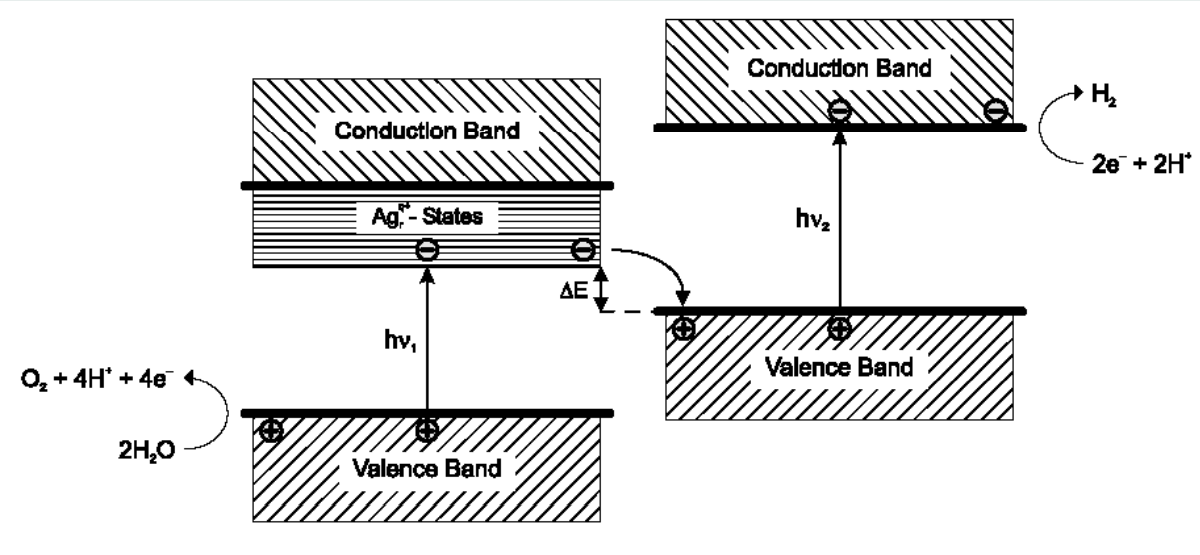
Grätzel, M. The artificial leaf, bio-mimetic photocatalysis. *Cattech* 3, 3–17 (1999).

22.10.2008

Nanochemistry UIO

24

Two-Photon Solar Conversion System



22.10.2008

Nanochemistry UIO

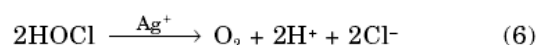
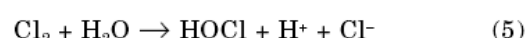
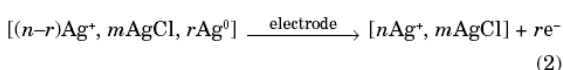
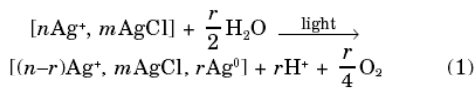
25

Silverclusters, Photography & Calzaferri Cell

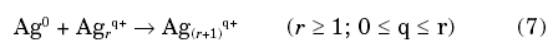
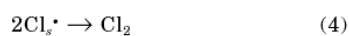
Quantum-Sized Silver, Silver Chloride and Silver Sulfide Clusters

JOURNAL OF IMAGING SCIENCE AND TECHNOLOGY® • Volume 45, Number 4, July/August 2001

Gion Calzaferri[▲], Dominik Brühwiler, Stephen Glaus,
David Schürch, Antonio Currao, and Claudia Leiggner



The Cl_s^\bullet radicals recombine very fast to form Cl_2 :



22.10.2008

Nanochemistry UIO

26

Silverclusters and Solar Conversion

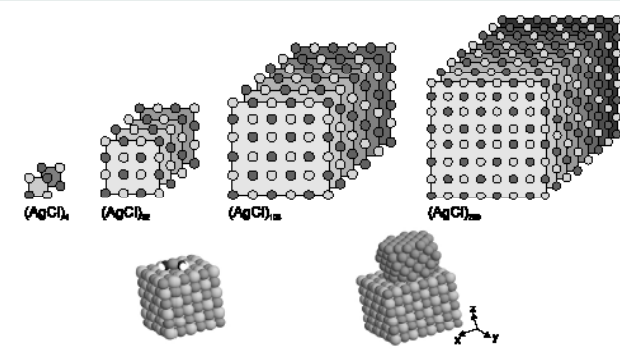
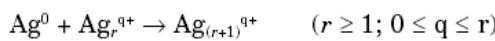
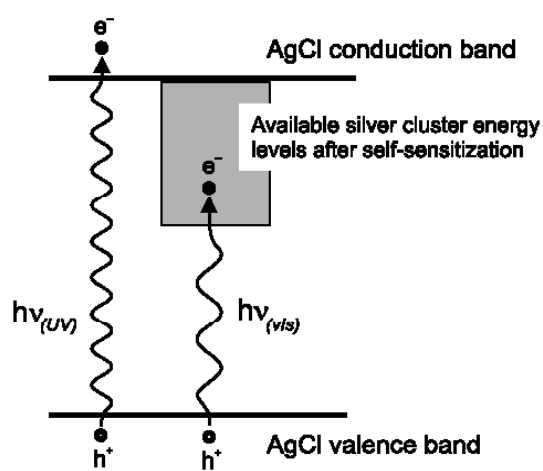
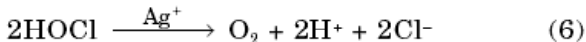
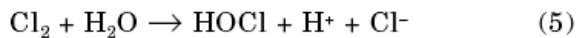


Figure 4. Clusters and composites discussed in this article. Top: $(\text{AgCl})_n$ clusters with (100) surfaces. Bottom left: the composite $(\text{Ag})_{115}(\text{AgCl})_{192}$. Bottom right: an adsorbed $\text{Ag}^+(\text{H}_2\text{O})_2$ on the surface of $(\text{AgCl})_{108}$.



22.10.2008

Nanochemistry UIO

27

Silverclusters and Solar Conversion

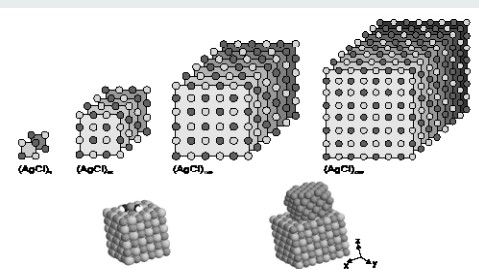


Figure 4. Clusters and composites discussed in this article. Top: $(\text{AgCl})_n$ clusters with (100) surfaces. Bottom left: the composite $(\text{Ag})_{115}(\text{AgCl})_{192}$. Bottom right: an adsorbed $\text{Ag}^+(\text{H}_2\text{O})_2$ on the surface of $(\text{AgCl})_{108}$.

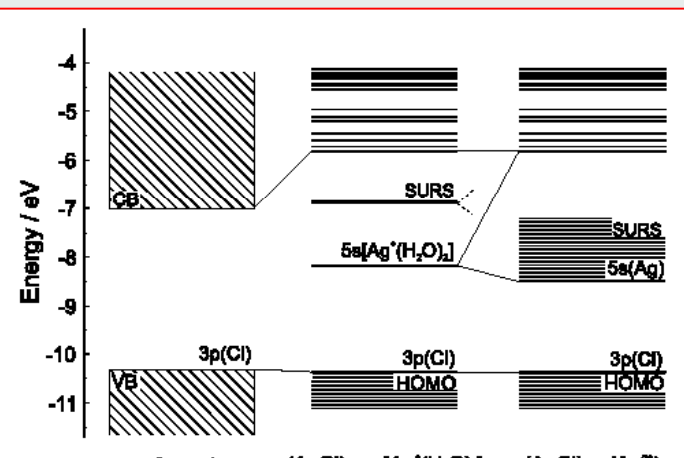
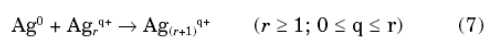


Figure 5. Comparison of the electronic structure of a silver chloride crystal, a silver chloride nanocluster with one $\text{Ag}^+(\text{H}_2\text{O})_2$ adsorbed on its surface, and one with several of them adsorbed (some of them already reduced and therefore represented as $(\text{Ag}_r^{q+})_{\text{aq}}$). The crystal band gap and $(\text{AgCl})_n-(\text{Ag}_r^{q+})_{\text{aq}}$ values correspond to experimental results.

22.10.2008

Nanochemistry UIO

28

Silverclusters and Solar Conversion

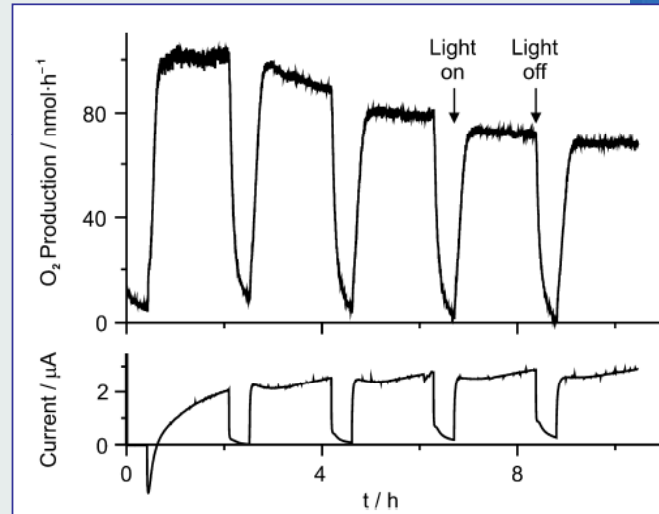
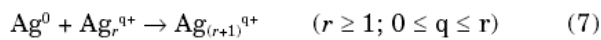
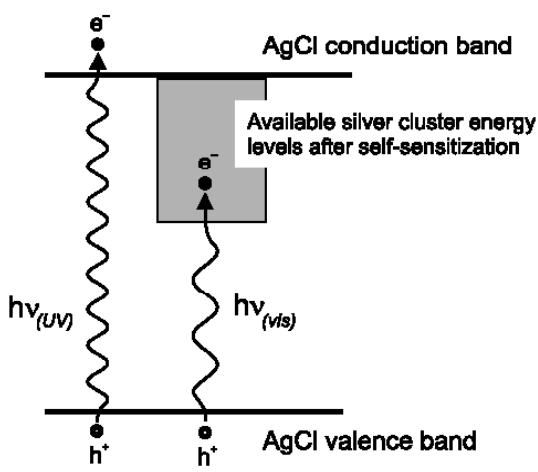


Figure 2. Chronoamperometry of a AgCl-coated $\text{SnO}_2:\text{F}$ electrode, carried out at 0.64 V versus NHE, with illumination and dark periods. The O_2 production rate ($\text{nmol}\cdot\text{h}^{-1}$) and the photocurrent (μA ; anodic current is drawn upwards) are plotted versus time.⁹

22.10.2008

Nanochemistry UIO

29

Flexible Thin Film Cells



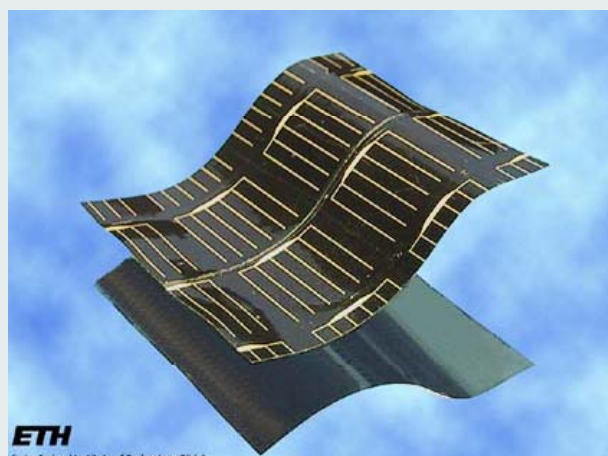
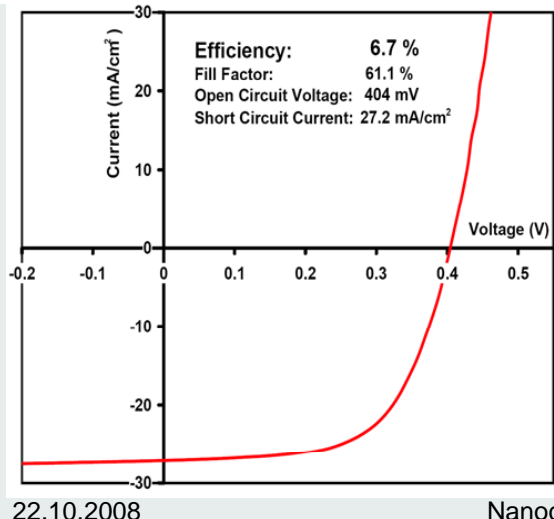
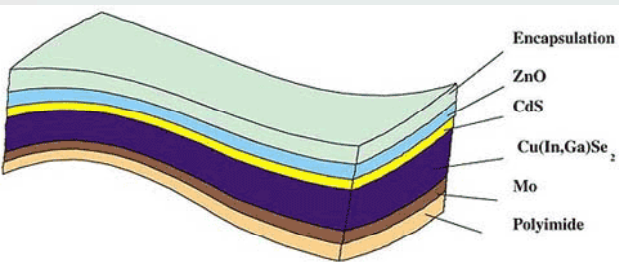
Flexible CIGS solar cells
 $\text{ZnO:Al}/\text{ZnO}/\text{CdS}/\text{CIGS}$ on $10 \times 10 \text{ cm}^2$ polyimide

Deposition possible on $15 \times 15 \text{ cm}^2$ polyimide

Further development

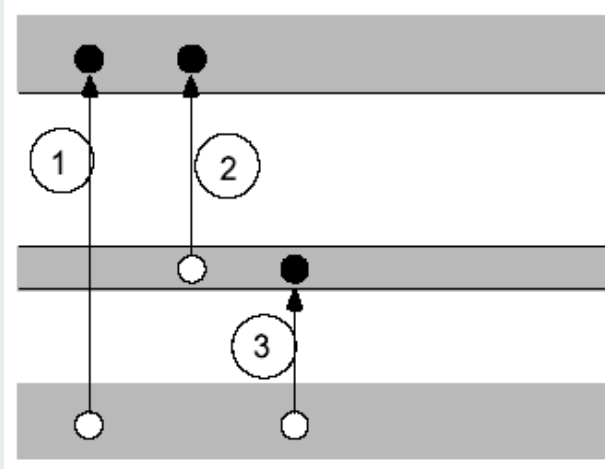
Scribing, process optimization, connections, encapsulation

Flexible Thin Film Cells



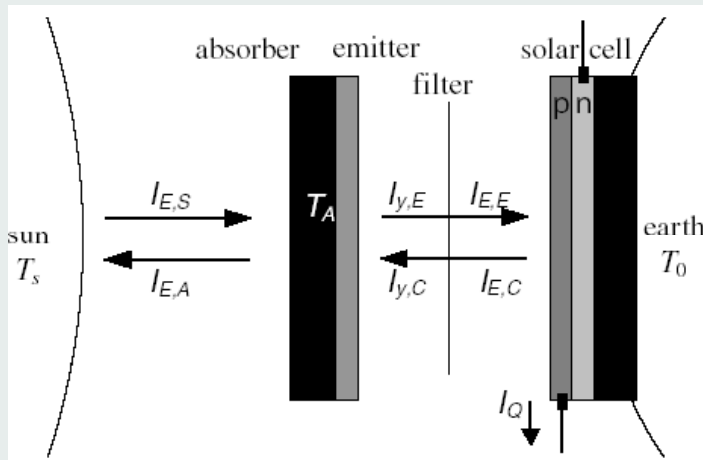
31

Multiband Cells



- Intermediate band formed by impurity levels.
- Process 3 also assisted by phonons
- Limiting efficiency is 86.8%

Thermophotovoltaic Cell



Burner:-
Burns fuel and heats up the emitter.

Emitter:-
Emits radiant heat energy.

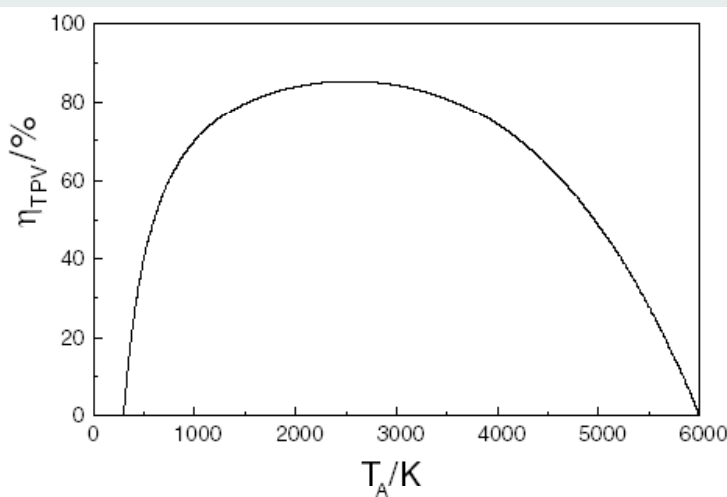
Filter:-
Selectively allows suitable radiation through to the PhotoVoltaic cell.

The remaining radiation is reflected back to the emitter to maintain the temperature and improve efficiency.

Thermophotovoltaic cell:-
the radiation incident on the cell causes a potential across the cell, just like in a solar cell but with heat radiation.

- Filter passes radiations of energy equal to bandgap of solar cell material
- Emitter radiation matched with spectral sensitivity of cell
- High Illumination Intensity (~ 10 kW/m²)

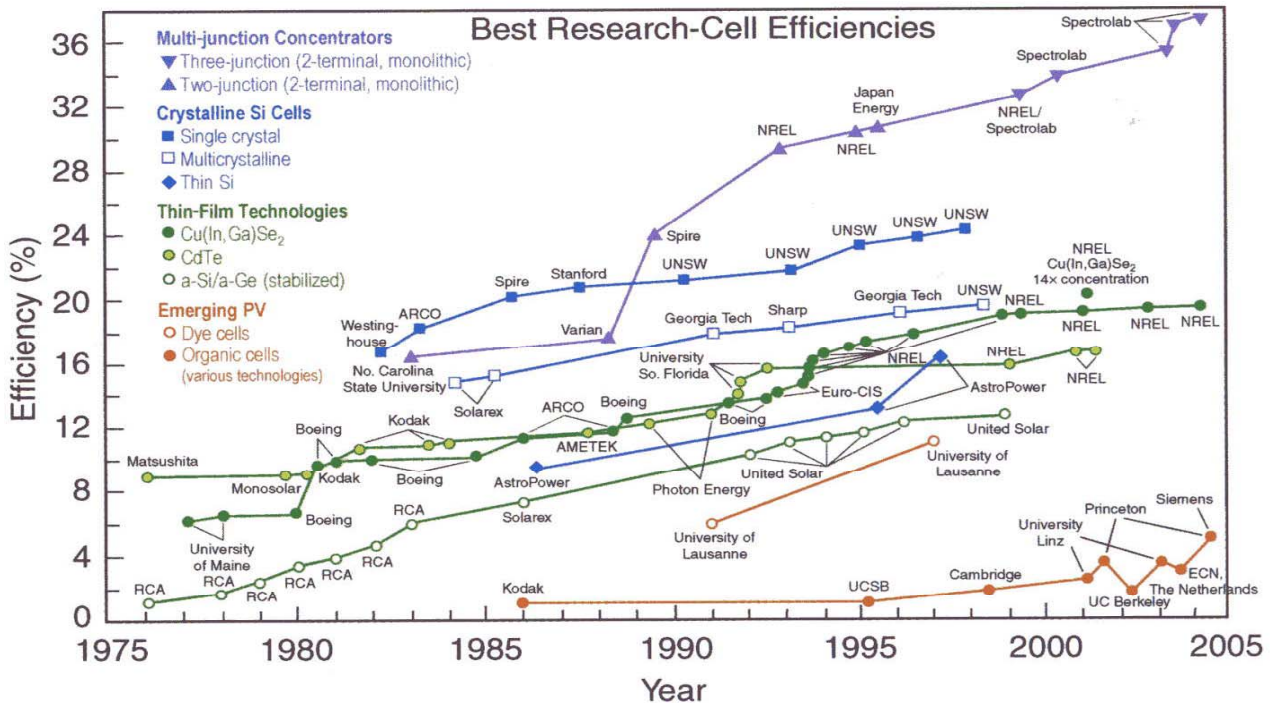
Thermophotovoltaic Cells



$$\eta_{\text{TPV}} = \left(1 - \frac{\pi}{\Omega_S} \frac{T_A^4}{T_S^4}\right) \left(1 - \frac{T_0}{T_A}\right)$$

- Efficiency almost twice of ordinary photocell

Present State of Cell Development

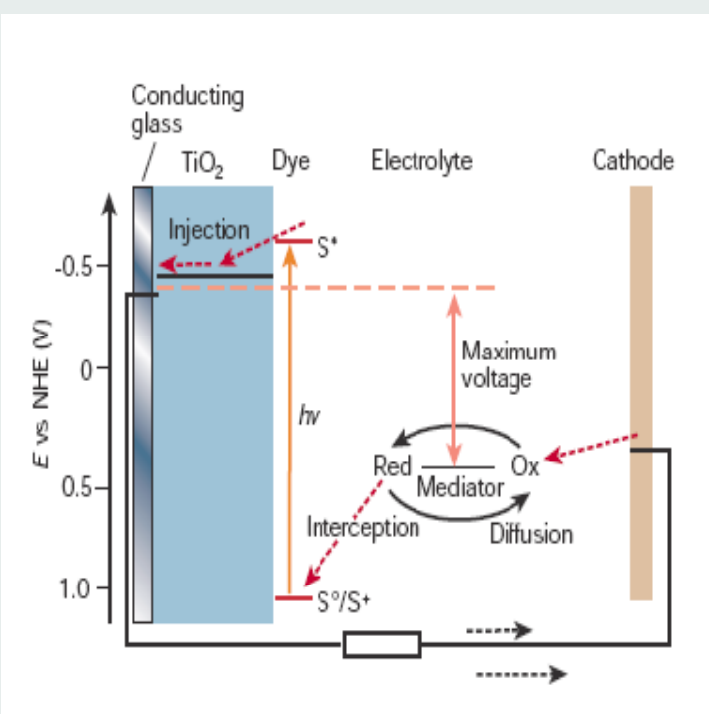


22.10.2008

Nanochemistry UIO

35

Solar Cell after M. Grätzel



22.10.2008

Nanochemistry UIO

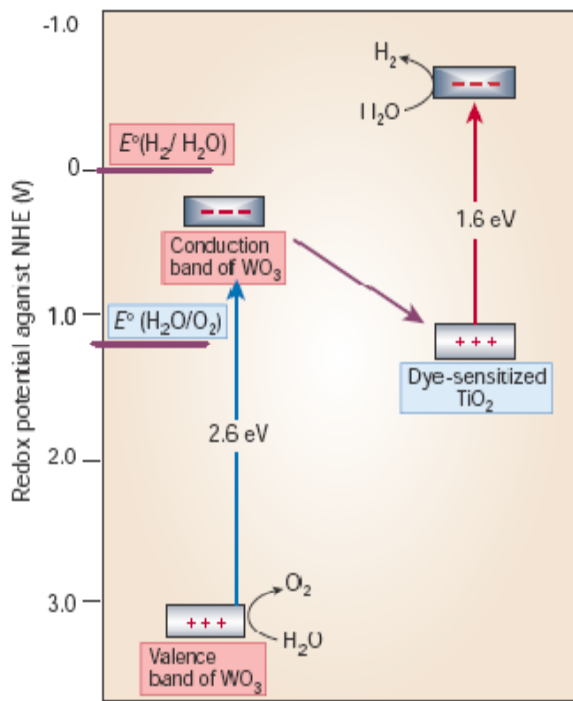
36

Tandem Cell for Water Cleavage

Based on two photosystems connected in series as shown in the electron flow diagram: A thin film of nanocrystalline tungsten trioxide, WO_3 (ref. 34), or Fe_2O_3 (ref. 35) serves as the top electrode absorbing the blue part of the solar spectrum. The valenceband holes (h^+) created by band-gap excitation of the film oxidize water to oxygen: $4\text{h}^+ + \text{H}_2\text{O} \Rightarrow \text{O}_2 + 4\text{H}^+$ and the conduction-band electrons are fed into the second photosystem consisting of the dye-sensitized nanocrystalline TiO_2 cell discussed above. The latter is placed directly under the WO_3 film, capturing the green and red part of the solar spectrum that is transmitted through the top electrode. The photovoltage generated by the second photosystem enables hydrogen to be generated by the conduction-band electrons.



The overall reaction corresponds to the splitting of water by visible light. There is close analogy to the 'Z-scheme' (named for the shape of the flow diagram) that operates in photosynthesis. In green plants, there are also two photosystems connected in series, one that oxidizes water to oxygen and the other generating the compound NADPH used in fixation of carbon dioxide.



Grätzel, M. The artificial leaf, bio-mimetic photocatalysis. *Cattech* 3, 3–17 (1999).

22.10.2008

Nanochemistry UIO

37

Present Solar Cells - Comparison

Type of cell	Efficiency (%)*		Research and technology needs
	Cell	Module	
Crystalline silicon	24	10-15	Higher production yields, lowering of cost and energy content
Multicrystalline silicon	18	9-12	Lower manufacturing cost and complexity
Amorphous silicon	13	7	Lower production costs, increase production volume and stability
CuInSe_2	19	12	Replace indium (too expensive and limited supply), replace CdS window layer, scale up production
Dye-sensitized nanostructured materials	10-11	7	Improve efficiency and high-temperature stability, scale up production
Bipolar AlGaAs/Si photoelectrochemical cells	19-20	—	Reduce materials cost, scale up
Organic solar cells	2-3	—	Improve stability and efficiency

*Efficiency defined as conversion efficiency from solar to electrical power.